University of Stavanger

Faculty of Science and Technology

MASTER'S THESIS

Study program/ Specialization: Petroleum Engineering/Drilling Technology	Spring semester, 2013 <u>Open</u> / Restricted access
Writer: Kurt Louis Krogsæter	…… (Writer's signature)
Faculty supervisor: Gerhard Nygaard	
Thesis title: Automatic Evaluation of Drilling Fluid Properties Conventional and MPD Operations	
Credits (ECTS):30	
Key words: Drilling fluid technology Instrumenal Circulation Path Drilling automation Differential-Pressure	Pages: 49 + enclosure: 10 Stavanger, 12/07/2013 Date/year

University of Stavanger

Master's Thesis

Automatic evaluation of drilling fluid properties during conventional and MPD operations

Author:
Kurt Louis Krogsæter

Supervisor:
Prof. Olav Gerhard H. Nygaard

Master of Petroleum Engineering

in the

Well Engineering
Department of Petroleum Technology

July 2013

UNIVERSITY OF STAVANGER

Abstract

Faculty of Science and Technology
Department of Petroleum Technology

Master of Petroleum Engineering

Automatic evaluation of drilling fluid properties during conventional and MPD operations

by Kurt Louis Krogsæter

The primary barrier to maintain well integrity in drilling operations is the drilling fluid. With the current routines of evaluating the fluid properties and the increasingly use of automated and advanced drilling technology, the margin of error could be fatal.

The main focus of this thesis is to evaluate if differential-pressure measurements could be used to continuously evaluate fluid properties. An experimental set-up was built with differential-pressure sensors across a horizontal and a vertical section. The density and the friction factor were then calculated regardless of laminar or turbulent flow. The test were performed with water.

During the testing phase, it was discovered that the pump characteristics were not accurate for very low flow rates. For higher flow rates the experimental set-up showed promising data values that could characterize the properties of water, but it still need further work to achieve reliable data...

Acknowledgements

This document concludes my studies as a masters student in Petroleum Technology at the University of Stavanger.

I was exited to take on the huge task that the project represented, and the process has been rewarding and a great learning experience. As a previous mechanic, I was able to utilize my skills in the building of the experimental set-up, and challenge myself in areas where I did not have any pre-existing knowledge.

A special thank to my supervisor, *Gerhard Nygaard*, for providing me with this interesting project. I would also like to thank *Sivert B. Drangeid* for suggestions when needed, and *Inger J. Olsen* for the cooperation of procurement of building materials at the *Institute of Petroleum Technology, UiS*.

Lastly I want to thank my fellow students through long working hours, and my friends and family during these 5 years at the University...

Contents

List of Figures

List of Tables

Physical Constants

acceleration of gravity $g = 9.81\ \mathrm{m}^2/\mathrm{s}$

Symbols

L	pipe length	m
h	pipe hight	m
D	pipe diameter	m
A	cross sectional area	m^2
P_p	pump pressure	Pa (kg/(m s^2))
P_d	hydrostatic pressure	Pa (kg/(m s^2))
P_d	dynamic fluid pressure loss	Pa (kg/(m s^2))
dP_{hor}	horizontal differential-pressure	Pa (kg/(m s^2))
dP_{ver}	vertical differential-pressure	Pa (kg/(m s^2))
V	velocity of the fluid	m/s
Q	flow rate	m^3s
Re	Reynolds number	
f_{lam}	frictional factor at laminar flow	
f_{turb}	frictional factor at turbulent flow	
ρ_l	density of liquid	kg/m^3
ρ_o	density of silicone oil	kg/m^3
ν	kinematic viscosity	m^2/s
μ	dynamic viscosity of the fluid	kg/(m s)
ϵ	roughness for drawn tubing	

Chapter 1

Introduction to the thesis topic

One of the main barriers to maintain well integrity in drilling operations is the drilling fluid. It is therefore desirable to have the fluid column in an overbalanced pressure-state in the well to prevent unintended influx of hydrocarbons. In today's oil and gas industry the pressure margins gets more and more narrow to reach the desired and available hydrocarbon reserves. Therefore the parameters of the drilling fluid, rheology properties and density, has to be carefully monitored.

With more marginal prospects and harsher climate the operations are located at, the oil and gas industry needs to advance their technology to overcome these challenges up ahead with respect to safety and environment. New and more complex drilling fluid components have been introduced such as high-viscosity pills, polymers, weighting materials and spacer fluids. These new additions to the drilling fluid creates an increased challenge of estimating the rheology and density of the fluid without a good knowledge of the substance. The current routine standard tests performed at the operation site is done manually. Density of the drilling fluid is usually controlled every 15 minutes at atmospheric pressure and temperature conditions. These estimation can be incorrect accordingly to the true data values of the fluid properties. Within the well there is a higher pressure and temperature environment, and this can lead to different rheology properties than measured at surface.

A more stable and accurate way of anticipating the rheology of the drilling fluid, is needed for the automated and advanced drilling technologies that are being used today. By replacing the manually routine test with introducing an automated continuous measurement test, can be very beneficial to automated well-control operations.

Carlsen [1] examined in her paper if it is possible to achieve constant on-line monitoring of dynamic viscosity and frictional factor through a pipe with differential-pressure sensor

across a pipe. Tests on a instrumental 20 meter horizontal 4 inch pipe indicated that this is highly feasible. The tests were performed at the IRIS Ullring drilling and well center test facilities.

1.1 Automated Drilling Hydraulics Laboratory

Previous students at the University of Stavanger have been developing and working with an experimental rig set-up for evaluating rheology and fluid properties automatically through an instrumented standpipe. The laboratory is a collaboration between the University of Stavanger, International Research Institute of Stavanger (IRIS) and partially founded by Statoil. The E-hall, Kjølv Egeland building, at the University of Stavanger is reserved for the Department of Petroleum Engineering, and that is where the laboratory for Automated Drilling Hydraulics Laboratory is located.

The first addition to the laboratory started in 2011 with Torsvik's Master thesis [2]. A small scale operating drilling rig was built with all the necessary functions. The rig model is built to simulate the circulation system used in real drilling operation, and are operated through a PC using Simulink. All necessary pressure and flow data from the flow loop can be monitored. Wang [3] contributed to further optimize the rig for emulating Managed Pressure Drilling. The most recent contribution on the rig was Hansen [4]. Two differential-pressure transmitters were implemented on the flow loop. The first transmitter were placed on the horizontal section and the second on the vertical stand pipe section with a distance of 0.855 meter. The last addition to the rig were to examine rheological parameters, fluid density and frictional parameters. The results given from the differential-pressure transmitters gave low quality data due to disturbance in signals.

1.1.1 Objective and Scope of Work

In 2012 Hansen [4] presented in his thesis the fundamentals of drilling fluid hydrodynamics, the three most commonly used rheology models, and the conventional way of testing the drilling fluid properties in the industry. Since this thesis is a follow-up on Eirik Hansen work, the fundamentals of drilling fluid technology will therefore not be included in this thesis.

This thesis is focused around how to achieve rheology properties of a fluid with differential-pressure readings in a flow path. So that real time data of fluid properties and rheology such as fluid density, viscosity, Reynolds number and friction parameters can be extracted from continuous measurements. More importantly, the objective is to test with

instruments that are capable to be used in the oil and gas industry. The differential-pressure transmitter consist of metallic diaphragms and capillary diaphragms seals containing silicon oil with known density. These diaphragms seals can be mounted directly to the flow line with a flange. This should provide the differential relationship between the capillary forces in the transmitter tubes and the liquid in the flow loop. Fluctuating fluid properties can then be continuous monitored, and thus avoid maintenance for cleaning out the capillary tubes to the transmitter.

This thesis presents:

1. The build of the new addition to the Automated Drilling Hydraulics Laboratory.
2. Experimental testing on the new Instrumented Circulation Path with water to verify if measurements are reliable accordingly to theoretical values.

Chapter 2

Theory

This Chapter will present a series of equations that have been used to determine the fluid rheology and density. Matlab models are also included for estimating theoretical values.

2.1 Pressure Loss Calculations

When calculating the pressure in a well it is necessary to have two parameters, the density and frictional properties of the drilling fluid. The drill-string pressure and the well-bore pressure have two main contributions, the hydrostatic pressure and the dynamic fluid pressure loss. The pressure loss is affected by the friction between the wall of the pipe and the drilling fluid flow. Frictional pressure loss is also influenced by other factors that are presented by the formulas in this Chapter.[5]

The assumption that has been taken in this thesis is that a Newtonian fluid are flowing through a pipe. This means no compensations for shear thinning and non-Newtonian viscosity is taken into account.

The pump pressure P_p is defined as

$$P_p = \rho_l g h \tag{2.1}$$

and also equal to the sum of the hydrostatic pressure P_h and the dynamic fluid pressure loss P_d.

$$P_p = P_d + P_h \tag{2.2}$$

In this case the hydrostatic pressure contribution is within the capillary tubes, and is measured in the vertical section. The differential-pressure sensors are a concealed chamber from the diaphragm seals to the transmitter, and the density of the silicone oil based fluid is given by the producer. The formula is then given by

$$P_h = \rho_o g h \tag{2.3}$$

where ρ_o is the density of the silicon oil, g is the gravitational force and h is the height of the vertical pipe length.

Further, the dynamic fluid pressure loss is measured between the differential-pressure in the vertical pipe section dP_{ver} and the differential-pressure in the horizontal pipe section dP_{hor}.

$$P_d = dP_{ver} - dP_{hor} \tag{2.4}$$

The average fluid velocity of the fluid through a pipe is defined as

$$V = \frac{Q}{A} \tag{2.5}$$

where Q is the flow rate from the pump and A is the cross sectional area of the pipe.

The Reynolds number, Re, gives a measure of the ratio of inertial forces to viscous forces. This ratio is dimensionless. The formula for a pipe flow is defined as

$$Re = \frac{VD}{\nu} \tag{2.6}$$

where ν is the kinematic viscosity. The Reynolds number can also be written as:

$$Re = \frac{\rho_l VD}{\mu} \tag{2.7}$$

This shows that the kinematic viscosity is a ratio between the dynamic viscosity μ and the density of the fluid.

$$\nu = \frac{\mu}{\rho_l} \tag{2.8}$$

The friction factor used in this thesis is the Darcy/Moody friction factor. For laminar flow can be calculated from the Reynolds number.

$$f_{lam} = \frac{64}{Re} \tag{2.9}$$

This equation is only used for Reynolds number Re < 2300. When the Reynolds number exceeds 2300, the fluid flow will enter a turbulent state. The following equation, the Haaland equation, is then

$$\frac{1}{\sqrt{f_{turb}}} = -1.8 \log_{10}[(\frac{\epsilon/D}{3.7})^{1.11} + \frac{6.9}{Re}] \tag{2.10}$$

where the ϵ is the absolute roughness in pipe.

Finally the theoretical friction loss can now be estimated with a known length of the pipe, L.

$$P_d = \frac{fL\rho_l V^2}{2D} \tag{2.11}$$

This will give an theoretical indication of differential-pressure values that are desirable to achieve during testing.

2.2 Fluid Properties Calculations

In order to determine the density and apparent viscosity of the fluid flowing through the pipe using only differential pressure sensors, it is necessary to reverse the equation series in the previous section. This has to be done in the following order.

Combining formula from (2.1) to (2.4) will then give the density of the liquid in the flow pipe ρ_l as shown.

$$\rho_l = \rho_o + \frac{dP_{ver} + dP_{hor}}{gh} \tag{2.12}$$

The density found here will be used further in the calculations to determine the friction factor. The Darcy friction factor is found using the equation:

$$f = \frac{2DdP_h}{\rho V^2 L} \tag{2.13}$$

Then the Reynolds number can be calculated. For laminar flow the equation (2.9) is solved for Re_{lam}.

$$Re_{lam} = \frac{64}{f} \tag{2.14}$$

When the flow regime is in a turbulent state the Haaland equation (2.10) has to be solved with respect to Re.

$$Re_{turb} = \frac{6.9}{10^{(\frac{1}{-1.8\sqrt{f}})} - (\frac{\epsilon/D}{3.7})^{1.11}} \tag{2.15}$$

From equation (2.7) the apparent viscosity can be written in the formula:

$$\mu = \frac{\rho V D}{Re} \tag{2.16}$$

2.3 Modelling in Matlab

The equations given in Section 2.1 were used to make a Matlab model to compute the expected values of the pipe friction. The Matlab code is included in Appendix C.

2.3.1 Theoretical Differential-Pressure Values

The plots below, Figure 2.1 to Figure 2.3, indicates the pipe friction that should be expected during the testing phase. It also shows flow rates that should be applied to stay inside the 0 - 100 mBar. These values should not be exceed, due to the range of the differential-pressure sensors. The multiple lines represent increased liquid viscosity. When the viscosity is increased, it can be seen on the plots that the pipe friction will increase accordingly at a given flow rate. From Figure 2.4 to Figure 2.6, it is observed the transition between laminar and turbulent flow at increased viscosity and flow rate.

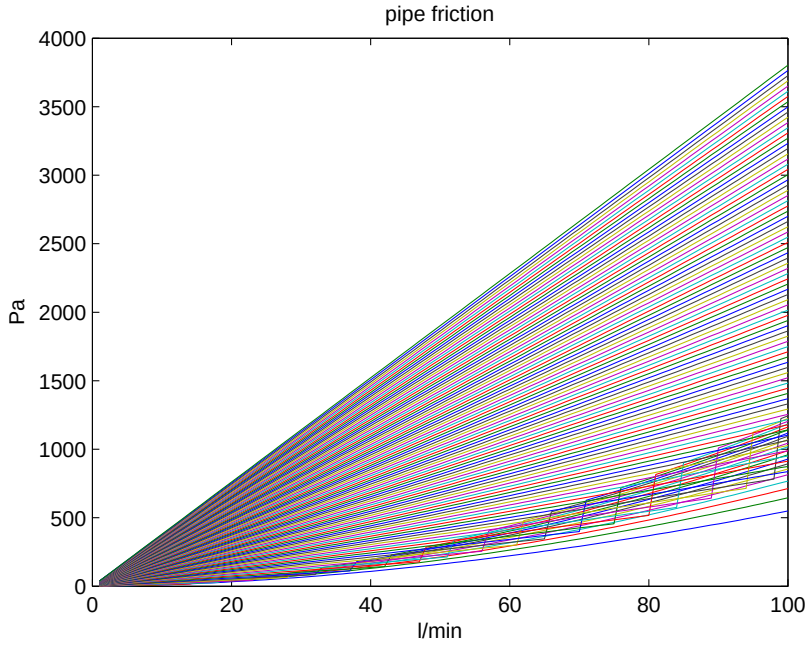

FIGURE 2.1: Pipe friction across the pipe at different flow rates for 50 mm pipe diameter

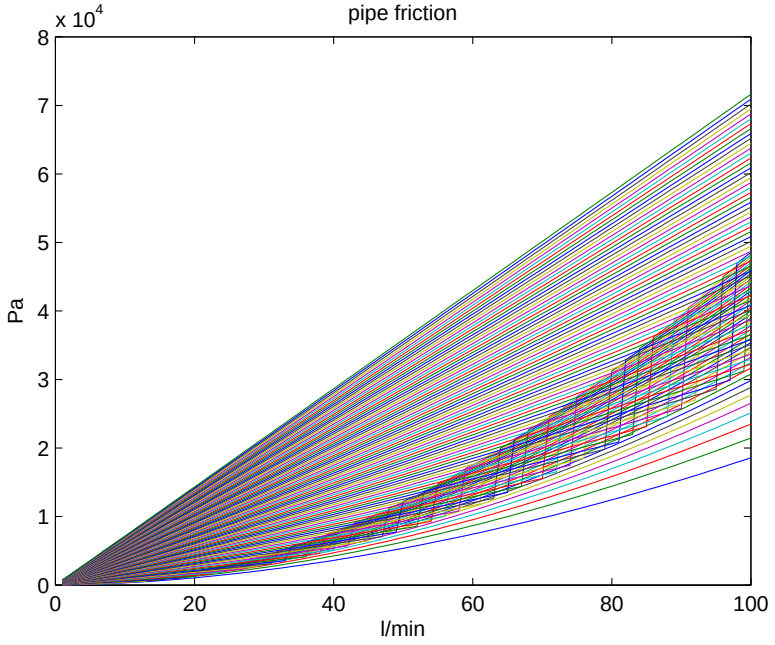

FIGURE 2.2: Pipe friction across the pipe at different flow rates for 24 mm pipe diameter

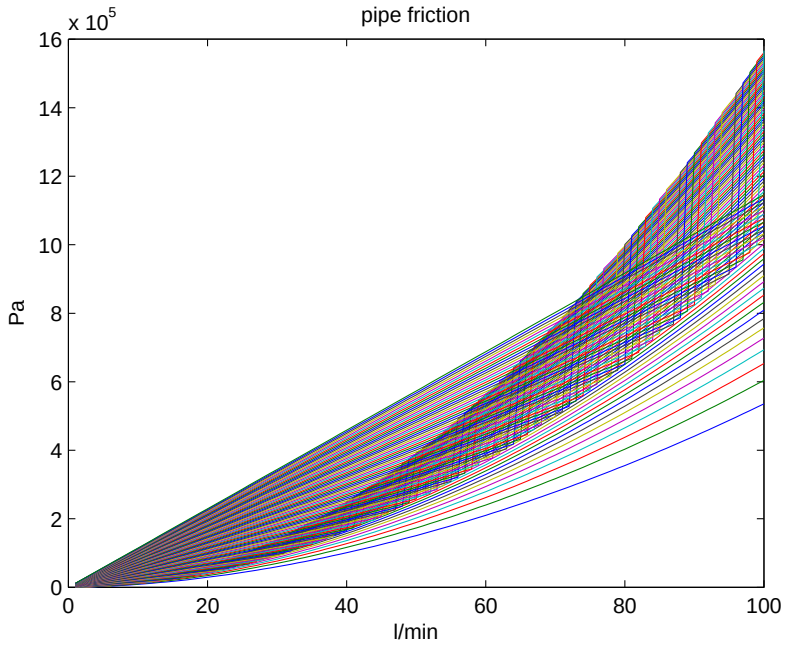

FIGURE 2.3: Pipe friction across the pipe at different flow rates for 12 mm pipe diameter

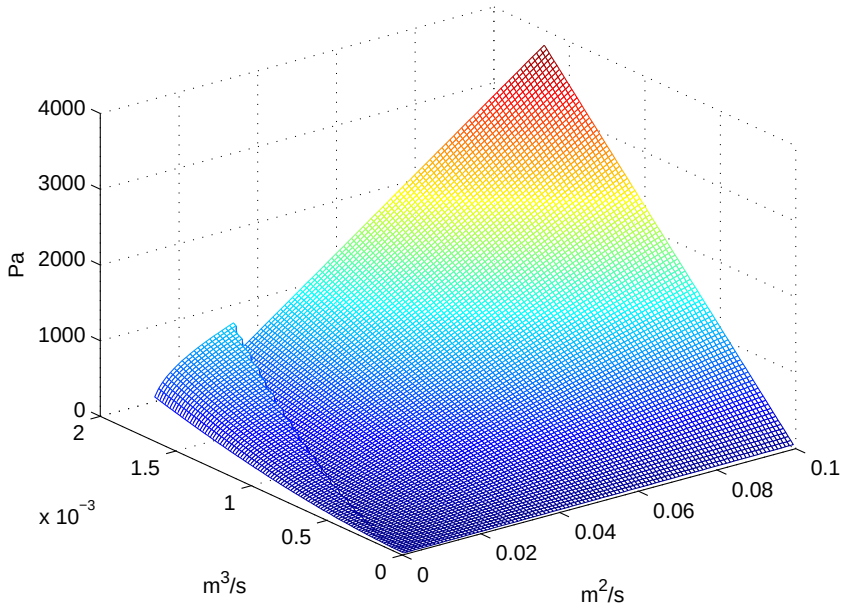

FIGURE 2.4: Relationship between headloss, flow rate and viscosity at 50 mm pipe diameter

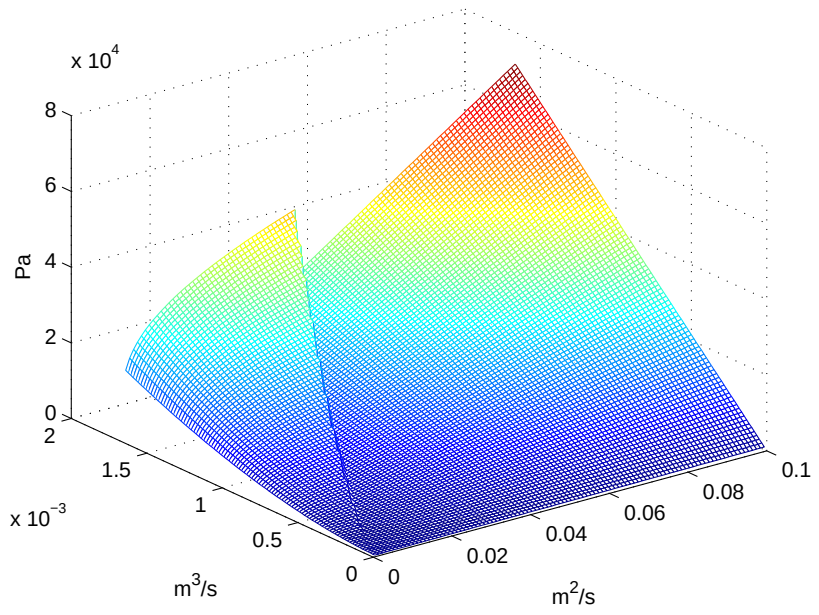

FIGURE 2.5: Relationship between headloss, flow rate and viscosity at 24 mm pipe diameter

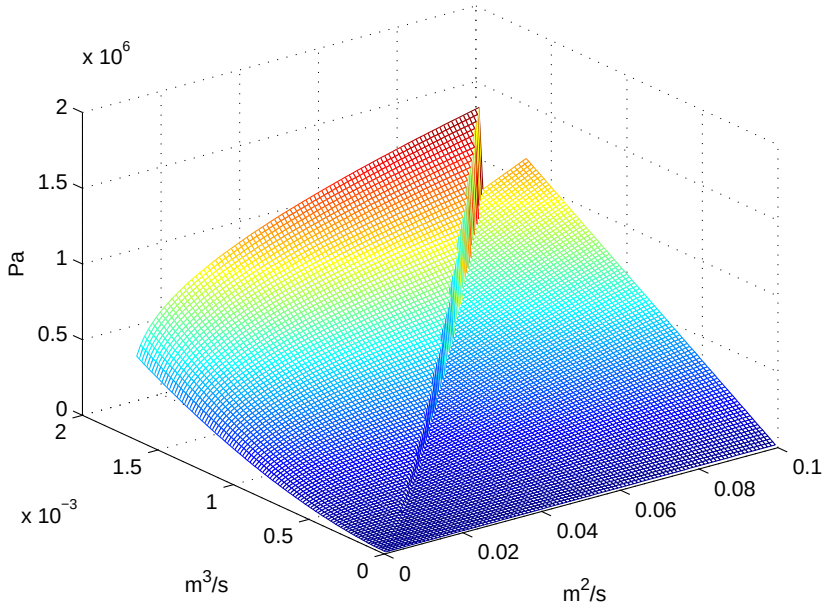

FIGURE 2.6: Relationship between headloss, flow rate and viscosity at 12 mm pipe diameter

Chapter 3

Building of the Instrumented Circulation Path

3.1 Planning Phase & Rig Set-Up

This project is a part of a laboratory facility for automated well control that is being built at the University of Stavanger. The project overview can be seen at Figure 3.1. The structures of this facility that has been finished is the flow loop that Torsvik [2] built during his Master thesis. This build represents the left side in Figure 3.1.

In this thesis it is planned to investigate and expand the facility with differential-pressure sensors in the return flow. To be able to start the build of the Instrumented Circulation Path, it would be necessary to do some planning ahead.

3.1.1 Research

The idea behind to monitor the return flow with differential-pressure, is to evaluate the drilling fluid properties automatically immediately the fluid returns from the well. This system can then detect attenuation influx by monitoring the drilling fluid rheology and properties, and automatically adjust the MPD Choke.

First of all, the desired sensors had to be able to read low differential-pressure, preferable 0-100 mBar. It should also be a sensor that can be used in the industry for real scale testing and use for stable measurements in harsh environments. After a while with researching the availability of sensors on the market, it was decided to order the DeltabarS FMD 78 from Endress+Hausser. Further details about the sensor is discussed in Section 3.2.2.

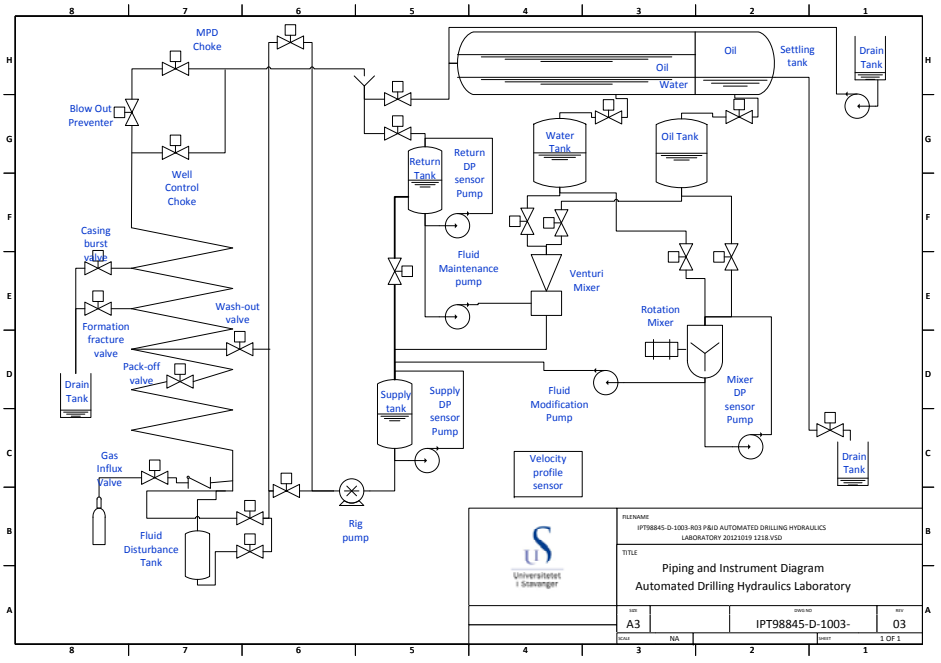

FIGURE 3.1: Automated Drilling Hydraulics Laboratory

It was also decided to use the existing pump at the laboratory, due to the time limit on the thesis. If new pump were to be ordered for this project, it has to have a stable pump characteristics for low pressure flow rates. The present pump at the laboratory were already connected to power supply and the control system that operates the flow loop. By modifying the outlet of the pump and the Simulink model that operates the pump, the pump could then be used for this project. The same tank as for the flow loop were also decided to utilize.

For the actual pipe line it was first planned to have just one pipe diameter at 12 mm for the circulation path. But after having several dialogues with the vendor of the differential-pressure sensors, it was recommended to increase the diameter of the pipe. The reason for this were because the smallest flanges for the metallic diaphragms came in DN50. It was advised to use pipe diameter of 50 mm or larger. This encountered a problem for the project. If the diameter had to be increased, meant that the length of the pipe had to be increased to achieve readable differential-pressure. Lack of space in the laboratory limited the horizontal pipe section to 3.5 m. After discussing the problem with the supervisor, it was decided to build three different pipe diameters to compare the results to each other. The three diameters were then 50 mm, 24 mm and 12 mm.

The pipes and pipe connections were purchased from local dealers in Stavanger for easy access of new parts if something were missing. Transparent pipes of 4 m were purchased from Crisma Plastic. Two sections for each pipe diameter, one for the horizontal section

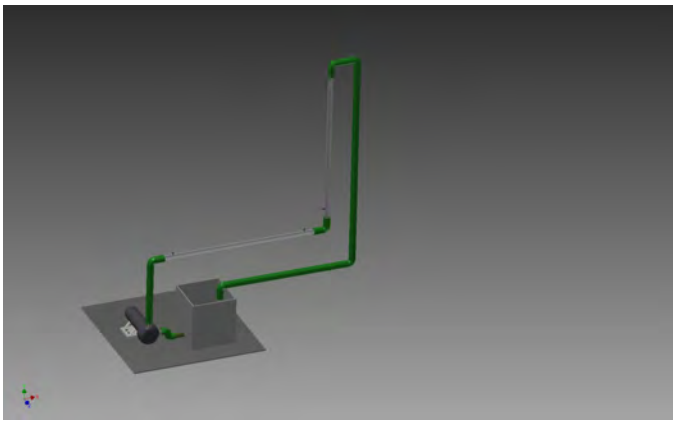

FIGURE 3.2: First draft of the Instrumental Circulation Unit

and the second for the vertical section. The bends and pipe connectors were purchased from Ahlsell. All pipe parts consists of PVC material.

Before actual purchasing all the necessary parts for the build, some Matlab scaling were performed to verify what input and output values could be expected. This is described in Section 2.3.1.

3.1.2 3D modelling

To get an idea of how the finished result is going to be, some models were made in Autodesk Inventor Professional 2013. This program can be purchased, or downloaded through the Autodesk Education Community for educational purposes[6].

The first sketch of the Circulation Path were made as seen in Figure3.2. This sketch were made before the dialogue with the differential-pressure vendor were taken place. The figure gives an basic illustration of how the set-up is going to be. A pump is connected to the bottom of the tank. The fluid will be distributes through a horizontal section before it is directed upwards to a vertical section, and the fluid is then returned back to the tank. Differential-pressure sensor are placed on both sections.

In the last part of the planning phase, some new sketches with three different flow paths of the Instrumental Circulation Path were created to have a clear illustration to work with. Figure 3.3 and Figure 3.4 are two options on how to distribute the flow in different paths. It was decided to use Figure 3.4 to reduce the flow disturbance created in the bends. The final concept drawing, Figure 3.5, will resemble the finished set-up.

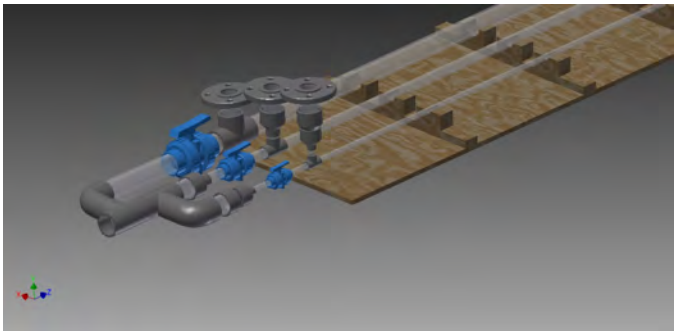

FIGURE 3.3: Pipe selector concept of the Instrumental Circulation Path

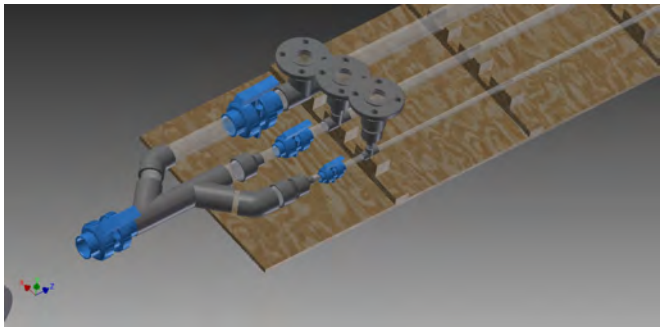

FIGURE 3.4: Final pipe selector concept of the Instrumental Circulation Path

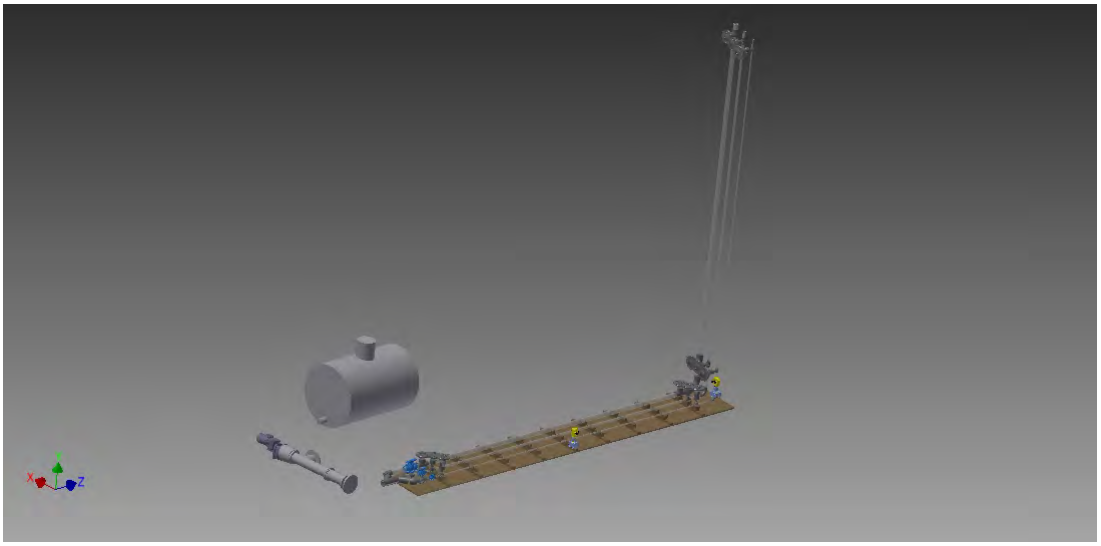

FIGURE 3.5: Final concept drawing of the Instrumental Circulation Path

3.2 Instrumented Circulation Path

This section will give a brief description of all components that have been used to build the Instrumented Circulation Path.

3.2.1 Building

The flow from the pump is directed through a tee, and the hose connects the flow to the Instrumental Circulation Path, as shown in Figure 3.6. The figure also shows a valve that must be closed at all time when operating the Instrumental Circulation Path. This is to prevent the fluid to go through another rig unit. Another important detail is the relief valve located beside the valve to prevent over-pressure in the system.

The pipe selector have three different flow paths. Only one path can be active at the time, because of there is only one differential-pressure sensor at each section. On the other side of the tee where the hose is connected there is a drainage system. Draining the system of liquid must be performed before changing to another flow path. Figure 3.7 will give a clear view of the system.

A small foundation of wood were made to attach the horizontal section. Since there are crane rails in the roof, the horizontal section had to be placed as low as possible. The vertical pipe section is mounted on a 4.5 m high sign post.

The first differential-pressure sensor is placed on the horizontal section, Figure 3.8, and the second on the vertical section illustrated on Figure 3.10. Both sensors are placed beneath the lowest measurement point according to the instructions for the sensors for best possible results, and are 3.5 m apart from each measurement point. The placement of the vertical sensor is seen on Figure 3.9. Hoses connected to the top of the vertical section will return the fluid back to the tank.

Operating procedures can be found at Appendix A.

3.2.2 Equipment Specifications

In order for the PC to send and receive correct signals, a series of electrical components is involved with the communication. The communication cabinate, Figure 3.11, distributes output and input signals from the PC to the desired target. This sub section will elaborate these different components.

FIGURE 3.6: Open/Close valve for directing the flow into the circulation path

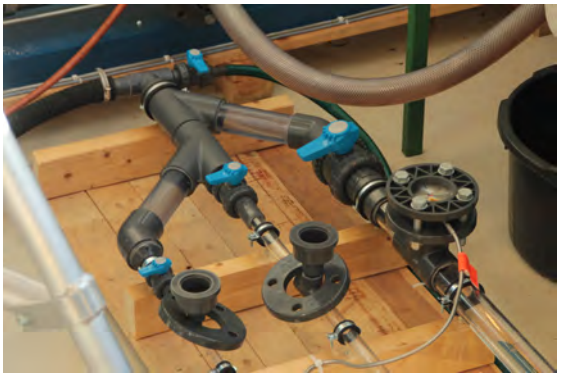

FIGURE 3.7: Pipe diameter selection and draining

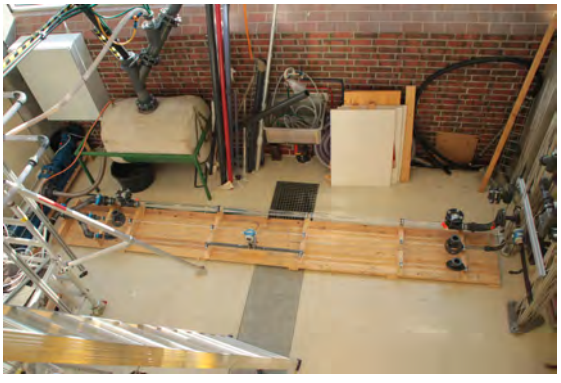

FIGURE 3.8: Overview picture of horizontal section

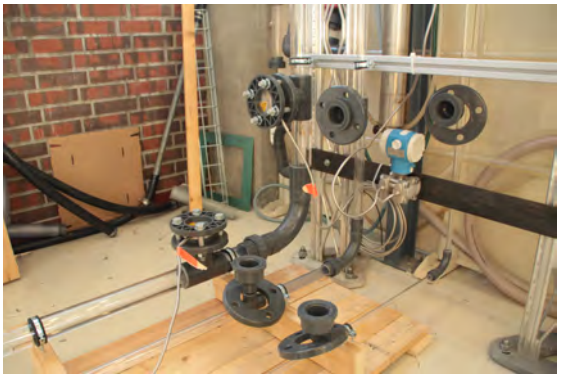

FIGURE 3.9: Connection between horizontal and vertical section

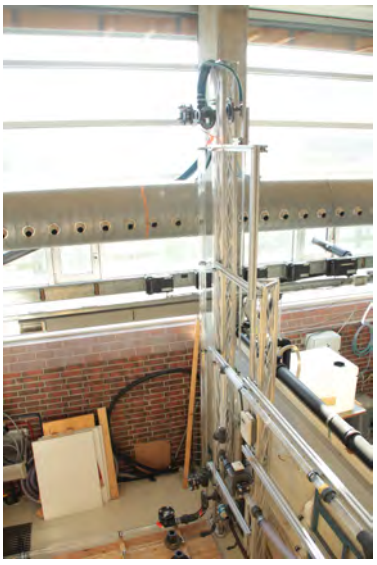

FIGURE 3.10: Overview picture of vertical section

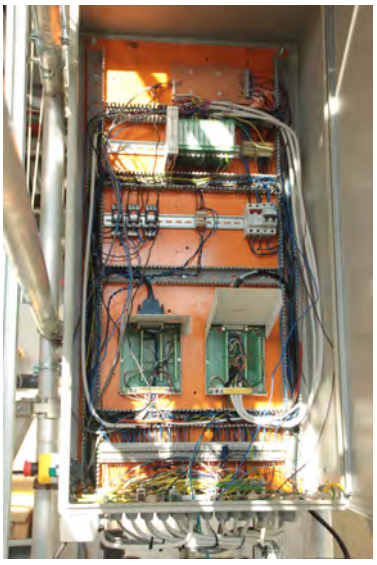

FIGURE 3.11: Communication cabinate

FIGURE 3.12: PCI box that communicates with the PC

3.2.2.1 PCI

There are two control cards in the communication box. One for the output signals(PCI 6703) and the second for the input signals(PCI 6221), Figure 3.12. These receive and send signals into the analogue input and output ports from the instruments and processes. The current they must receive and send is a 0-10 voltage signal. The computer operator that uses Simulink communicates with the PCI boxes made by National Instruments, and enables communication with the desired target.

3.2.2.2 Isolating Amplifier

Since the output signal from the differential-pressure sensors gives 4 - 20mA, they need to be converted into 0-10V for the PCI boxes to understand the right input signal. This is done by adding a isolating amplifier between the output signal from the differential-pressure sensors and the PCI (6221) box. They are powered by 24 V and separates the signals with a galvanic isolation. This isolation acts as a resistor. Four new isolating amplifiers were added to the communication box to transform the signals, Figure 3.13. See Appendix B

3.2.2.3 Motor and Tank

The manufacturer of the screw pump is PCM. Maximum flow rate that the pump delivers is 14 m^3/h. When adjusting the pump rate in Simulink, it will be given as % of maximum pump capacity. The equation between % and mass rate [kg/h] is shown in equation (4.1).

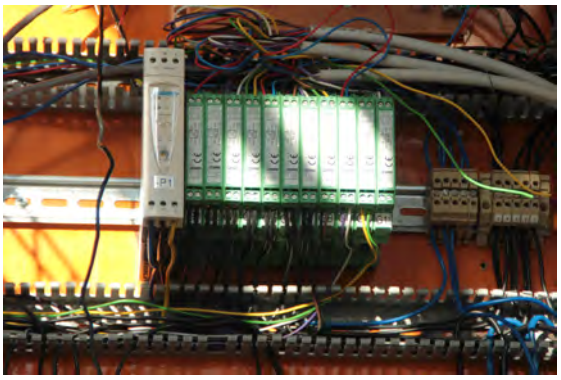

FIGURE 3.13: Signal converter from 4..20mA to 0-10V

FIGURE 3.14: Connection from the pump to the circulation path

At Figure 3.14 shows the suction point from the tank and outlet point of the pump. The tank capacity is 300 l, and are located besides the pump. It is filled with water.

3.2.2.4 Differential Transmitters

The DeltabarS FMD 78, Figure 3.17, is delivered by Endress+Hauser. These are a differential-pressure sensor with metal process isolating diaphragms and capillary diaphragm seals. An illustration of the diaphragm is shown in Figure 3.15. The field of application is liquid level and differential-pressure. In this case the differential-pressure application is used. Reference accuracy is up to ± 0.075% of the set span. The filling oil in the purchased sensors is equal to $\rho = 960$ kg/m ^{3}. The measuring range lies from -100 to + 100 mBar, and the adjusted measuring range 0 to 100 mBar. They give a signal output of 4-20mA HART. The ordered DeltabarS FMD 78 is mounted with a DN 50 flange connected at two points on each pipe section. The DN 50 flange is assembled on top of a tee, this is shown in Figure 3.16.

FIGURE 3.15: Diaphragm seal

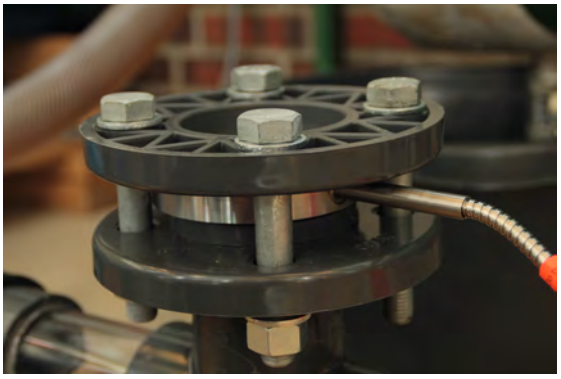

FIGURE 3.16: Mounted diaphragm seal

FIGURE 3.17: DeltabarS FMD 78 sensor

3.3 Simulink Model

To get the real time data received from the DeltabarS, Simulink had to be modified. Some changes were made in an existing Simulink file on the computer, now saved as "difftest". The changes are two new input signal from the PCI (6221), Figure 3.18. The new additions to the PCI (6221) analogue input can be found in Appendix B. It is also implemented real time data of fluid density, friction factor, Reynolds number and viscosity with the formulas computed at Section 2.2. The overlay of the computed fluid properties can be seen at Figure 3.19.

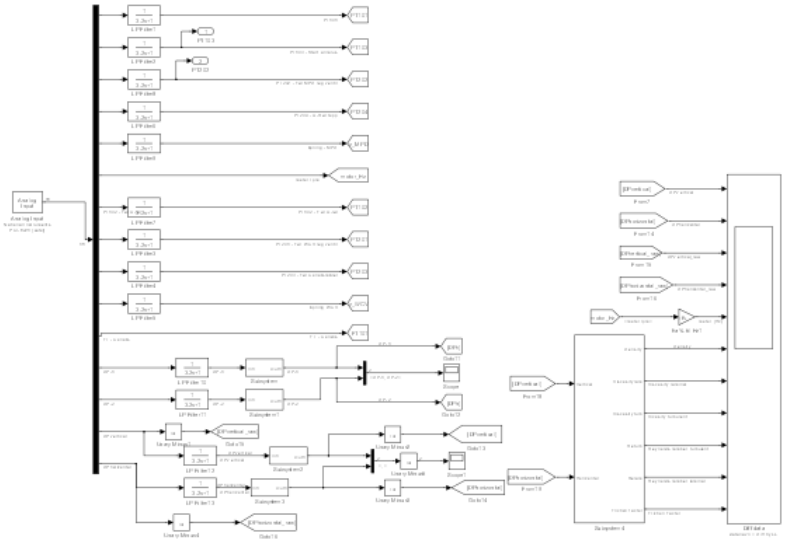

FIGURE 3.18: Output signals in Simulink

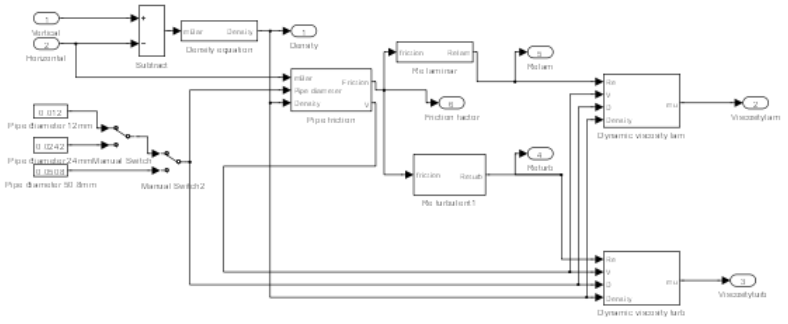

FIGURE 3.19: Computation of fluid properties in Simulink

Chapter 4

Details of experiment

4.1 Experimental Data

Results given from this experimental set-up were to investigate if it is possible to determine the fluid properties at a given flow rate. The tests were performed on three different pipe diameters, 50 mm, 24 mm and 12 mm. Water were pumped directly through the pipeline and returned back to the tank. The pipeline consists of a horizontal section and a vertical section. On each section there was placed a differential-pressure sensor with a distance of 3.5 meter apart. It was used a tee to connect the flange to the pipeline for the diaphragm. The differential-pressure sensors has a range of -100 to 100 mBar, and the adjusted measuring range had a setting of 0 to 100 mBar. Pump settings were controlled from the computer located at the laboratory.

The goal here was to see if fluid properties could be verified on a well known liquid with differential-pressure readings. Also, the differential-pressure sensors are equipped with metallic measuring diaphragms and capillary diaphragms seals. This forms a closed system from the measure point on the pipe to the transmitter. The process isolating diaphragms are deflected on both sides by the acting pressure in the pipe. The oil inside the capillary tubes transfers the pressure to a resistance bridge. This is based on the semi-conductor technology. The changes in the bridge gives an output of voltage which depends on the differential pressure.

A total of 12 individual tests were performed distributed on the three pipe diameters. All readings presented in this section had a time step of 0.0147 seconds. This is approximately 69 readings per second. Each test were performed with a constant flow rate which is represented in the tables respectively. The raw data from the differential-pressure sensor are used to estimate the fluid properties as seen in Chapter 2.

The pump have a maximum pump rate of 14 m^3/h, and the motor is regulated by percentage of maximum pump rate on the computer. The relationship between pump rate at 0 % to 100 % is then

$$Q = \% \text{ of maximum pump rate} \times \frac{14}{3600} \tag{4.1}$$

to convert the flow into m^3/s.

4.1.1 Differential Pressure Tests Through 50 mm Pipe

For the 50 mm pipeline it was performed 5 individual tests at different flowrates as seen in Table 4.1. Results from the Simulink model will give a direct reading of the differential-pressure, density of the fluid, friction factor, Reynolds number and the viscosity of the fluid. Figure 4.1 and 4.3 will show the direct voltage received from the differential-pressure sensor without any filtering. The time range for the data sets is between 0 s to 140 s. To convert the voltage readings to mBar, the signal goes first through a $\frac{1}{3.2s+1}$ low-pass filter then multiplied with 10. The mBar are then computed for the the horizontal- and the vertical-section as seen on Figure 4.2 and Figure 4.4, respectively. It can be observed that the hydrostatic pressure contribution is around 10 mBar. This is a bit below the expected value, thus will give a lower density than calculated. This are the raw data that has been used to evaluate fluid properties together with the output signal to the motor pump.

% of maximum pump rate	0.04	0.1	0.2	0.3	0.4
color	purple	blue	green	red	cyan

TABLE 4.1: Colors represent the different flow rates in 50 mm diameter pipe

Data collected from the 50 mm pipe line shows fairly stable measurements for low pressure losses. The density, Figure 4.5, shows an average data value of 990 kg/m^3. This is only 10 kg/m^3 below the real density of water. Further on the friction factor and the Reynolds number is presented for the individual pump rates. The data can be seen in Figure 4.6 and Figure 4.7 respectively. The last plot for the 50 mm diameter pipe, Figure 4.8, represents the viscosity of the fluid. It can be concluded that measurements with the color cyan and red can be discarded as good data. These two tests are the ones with the highest pump rate. Comparing the resulting data sets it can be observed that the average viscosity is in the range of ≈ 0.001 kgm^{-1}s^{-1} at time 100 s.

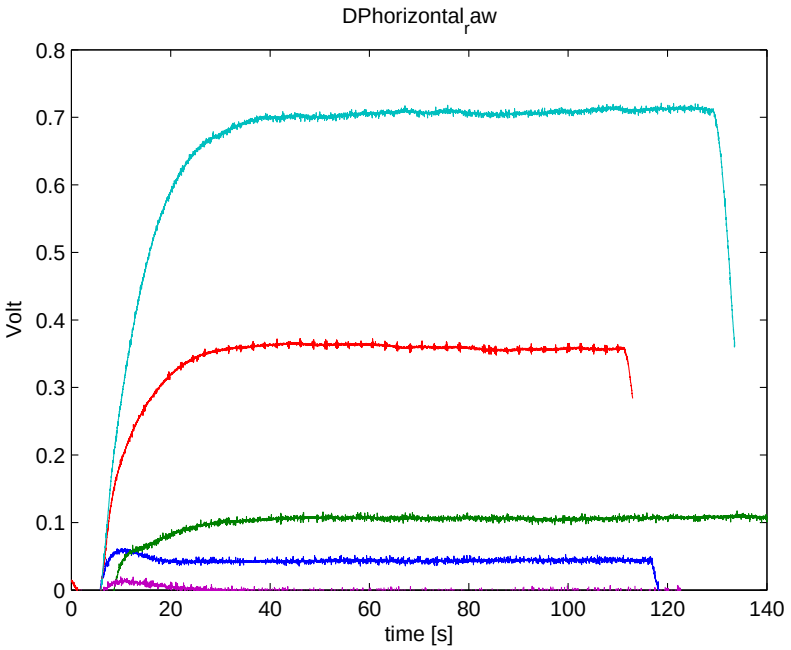

FIGURE 4.1: Voltage readings in horizontal line 50 - mm pipe diameter

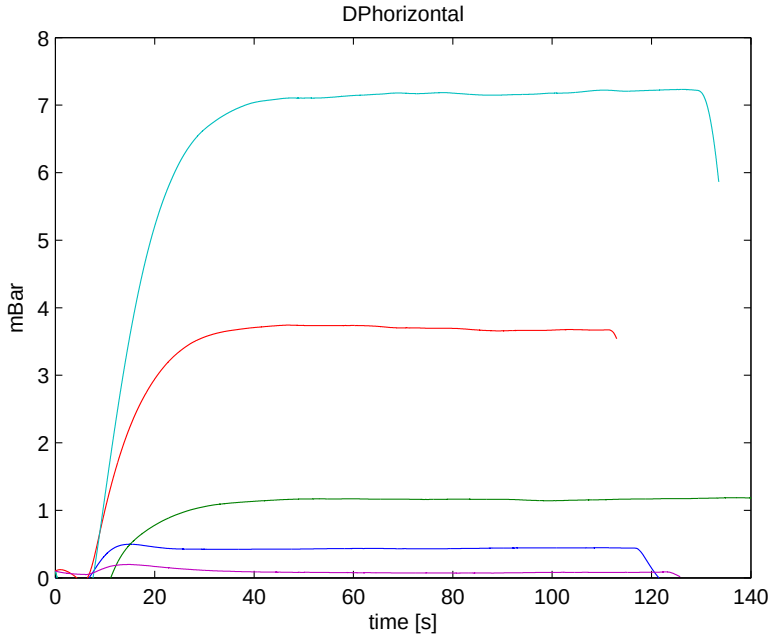

FIGURE 4.2: mBar in horizontal line 50 - mm pipe diameter

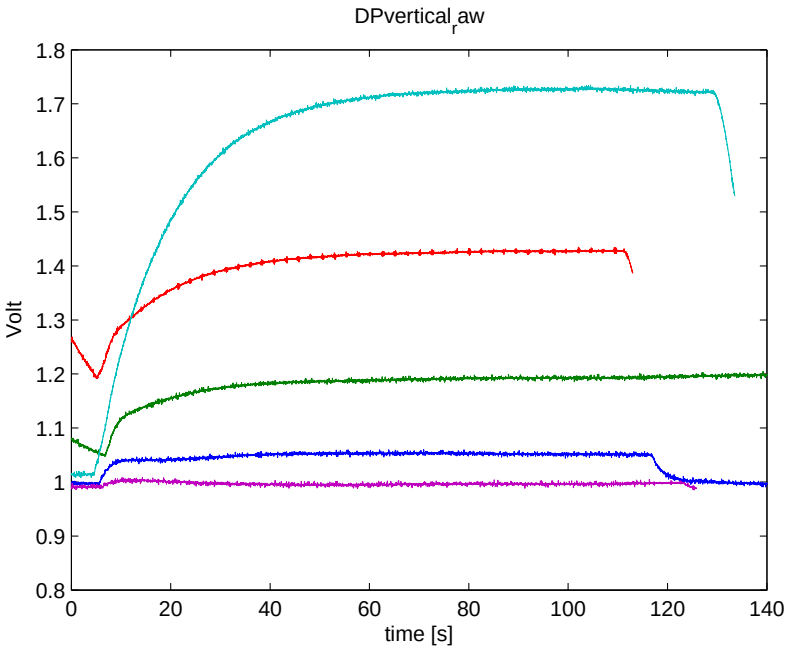

FIGURE 4.3: Voltage readings in vertical line - 50 mm pipe diameter

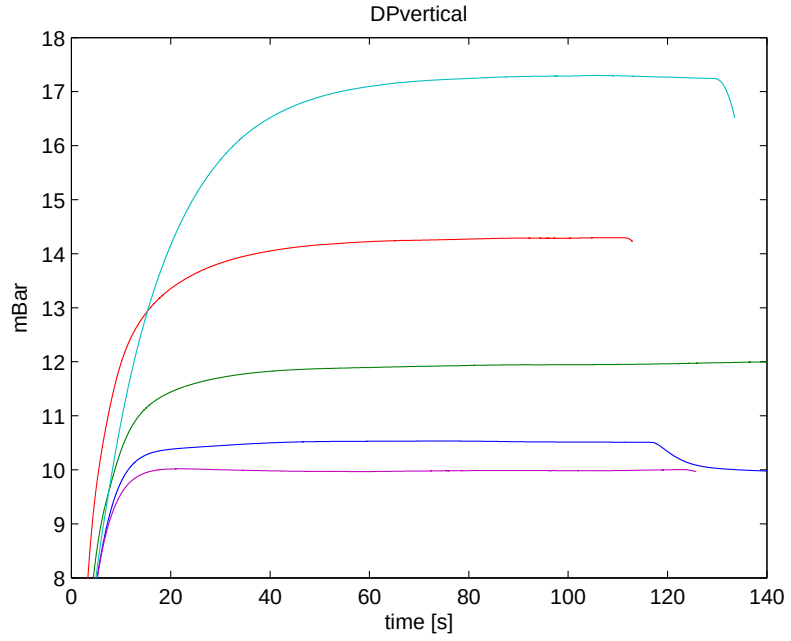

FIGURE 4.4: mBar in vertical line - 50 mm pipe diameter

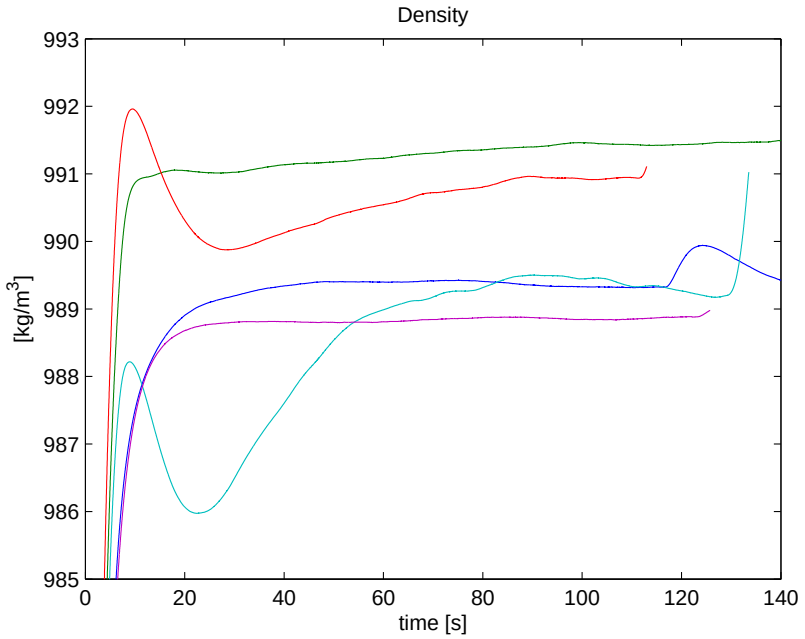

FIGURE 4.5: Density readings - 50 mm pipe diameter

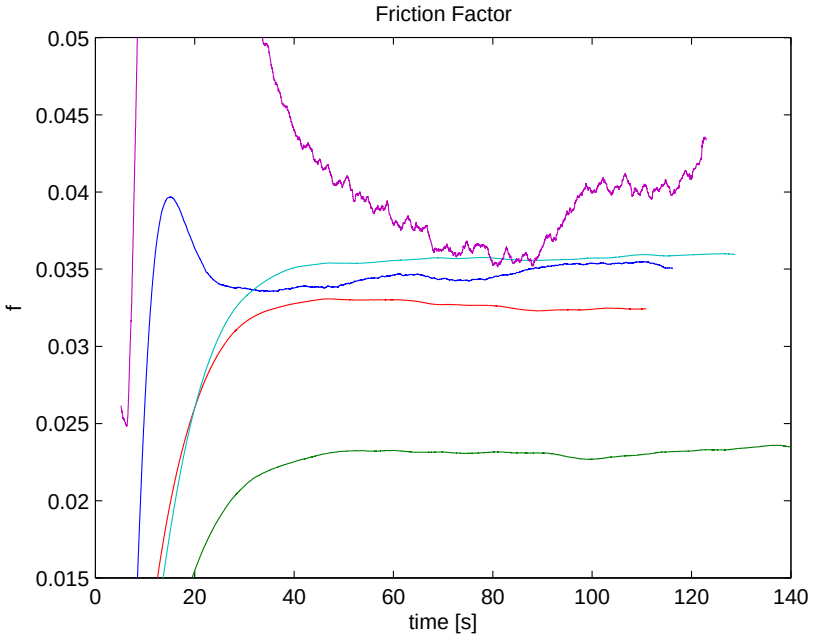

FIGURE 4.6: Friction factor readings - 50 mm pipe diameter

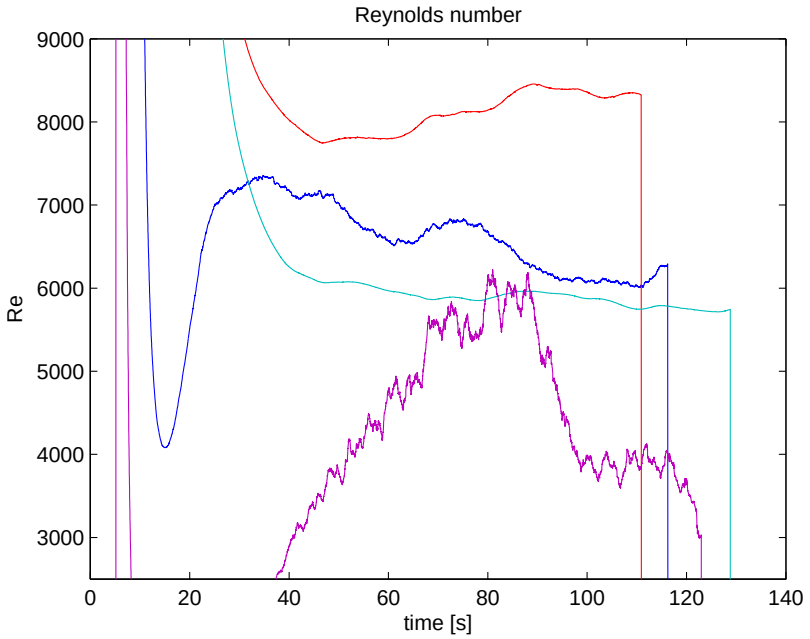

FIGURE 4.7: Reynolds number readings - 50 mm pipe diameter

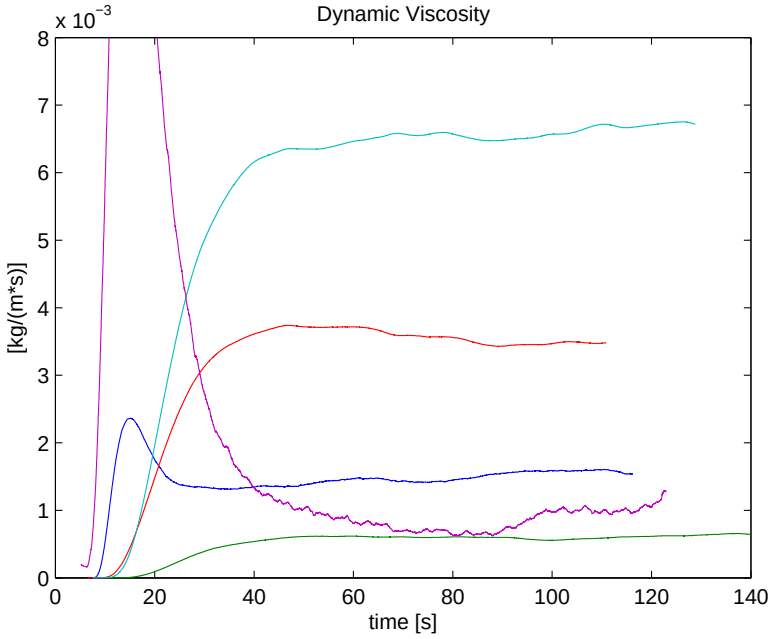

FIGURE 4.8: Dynamic viscosity readings - 50 mm pipe diameter

4.1.2 Differential Pressure Tests Through 24 mm Pipe

For the 24 mm pipe it was performed 4 measurements. The different flow rates are represented in Table 4.2. Since the sensor range of the differential-pressure sensor is set to 100mBar, the maximum pump pressure can not exceed 0.2% of maximum delivery rate of the pump. This is equal to 2.8 m^3/h. The time range of the recorded data is varying from 60 sec to 120 sec.

% of maximum pump rate	0.05	0.1	0.15	0.2
color	cyan	blue	red	green

TABLE 4.2: Colors represent the different flow rates in 24 mm diameter pipe

Figure 4.9 and Figure 4.11 represents the raw data from the Deltabar S sensor from all four data samples. No disturbance has been observed in the signals. The following plots for mBar measurements at the horizontal section and the vertical section is represented by Figure 4.10 and Figure 4.12, respectively. At this pipe diameter the density is varying from 1015 kg/m^3 to 995 kg/m^3, Figure 4.13. This indicates a slightly better approach to the theoretical value of water, but it has a bigger spread than it did for the 50 mm pipe diameter. The friction factor, Figure 4.14, gave a higher value than calculated. This resulted in a lower Reynolds number, Figure 4.15. Studying the plot of viscosity, Figure4.16, will point out that for the pump rate of 0.05% gave very low viscosity values and can therefore be discarded. The remaining data sets have a value between 0.001 $kgm^{-1}s^{-1}$ to 0.00145 $kgm^{-1}s^{-1}$.

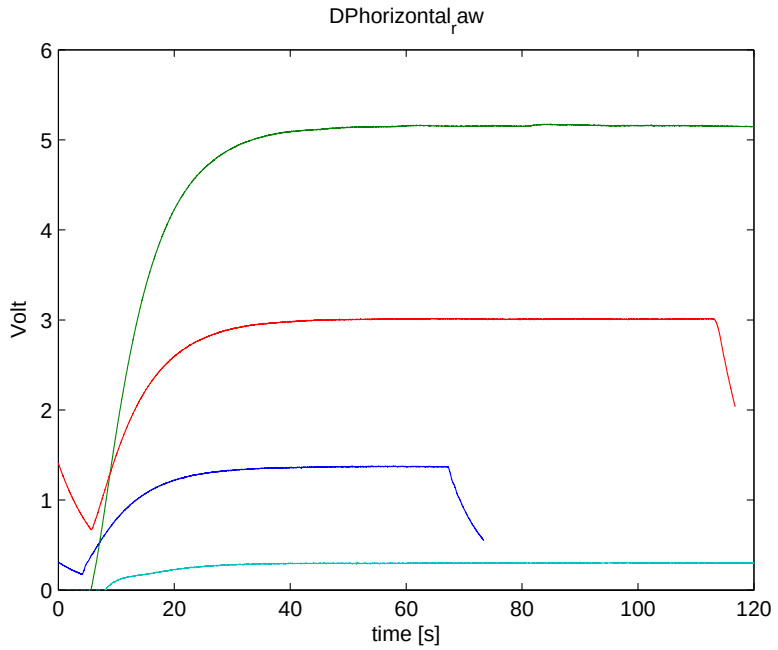

FIGURE 4.9: Voltage readings in horizontal line 24 - mm pipe diameter

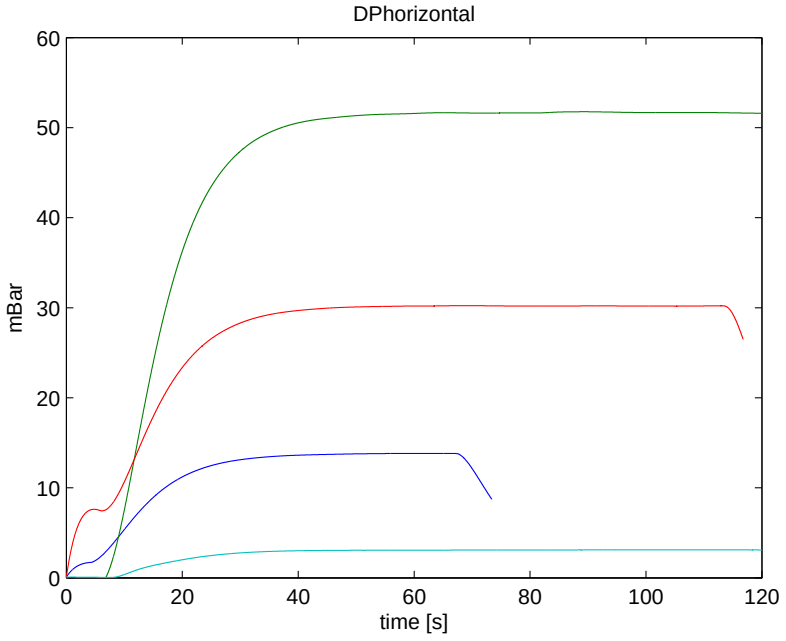

FIGURE 4.10: mBar in horizontal line 24 - mm pipe diameter

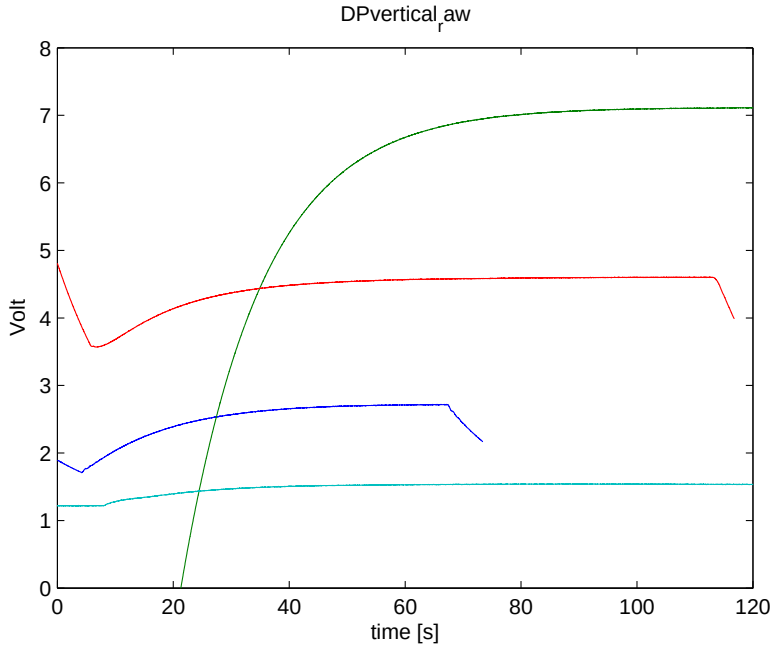

FIGURE 4.11: Voltage readings in vertical line - 24 mm pipe diameter

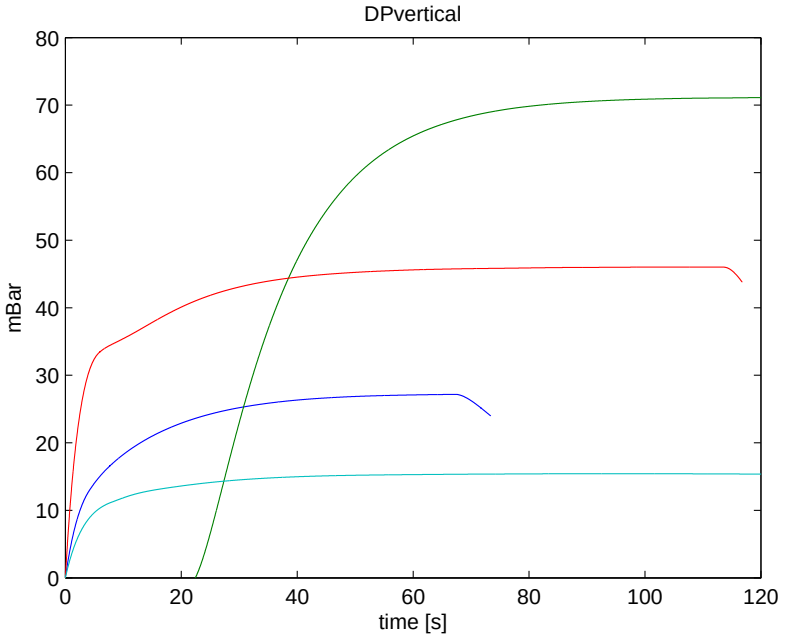

FIGURE 4.12: mBar in vertical line - 24 mm pipe diameter

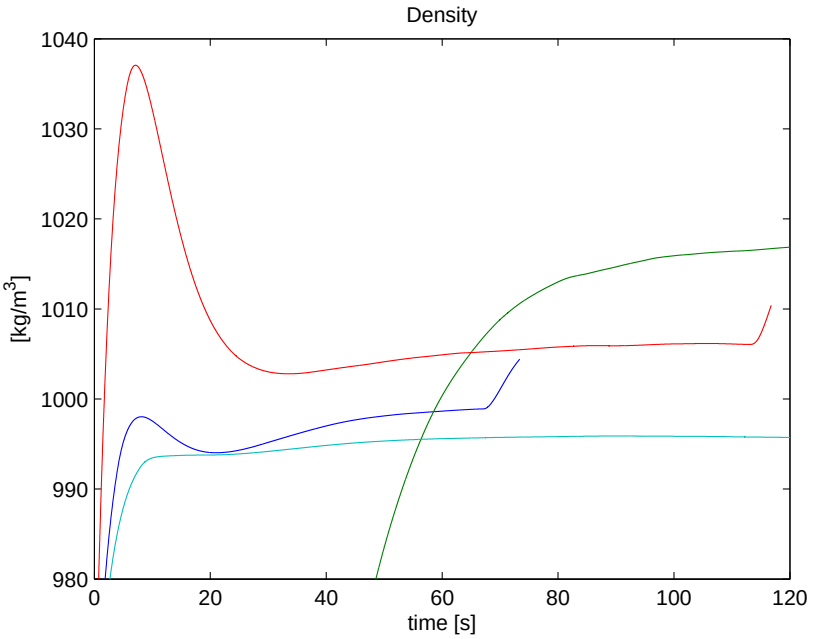

FIGURE 4.13: Density readings - 24 mm pipe diameter

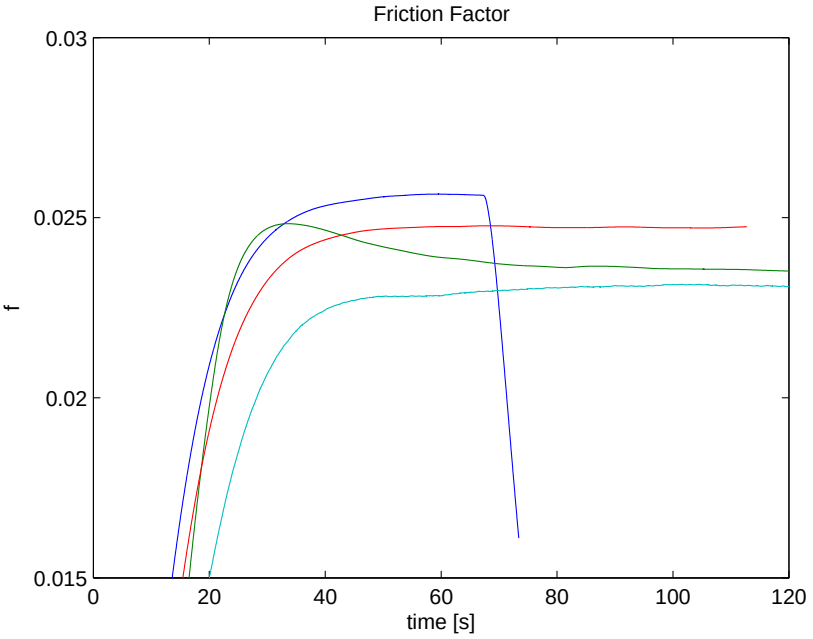

FIGURE 4.14: Friction factor readings - 24 mm pipe diameter

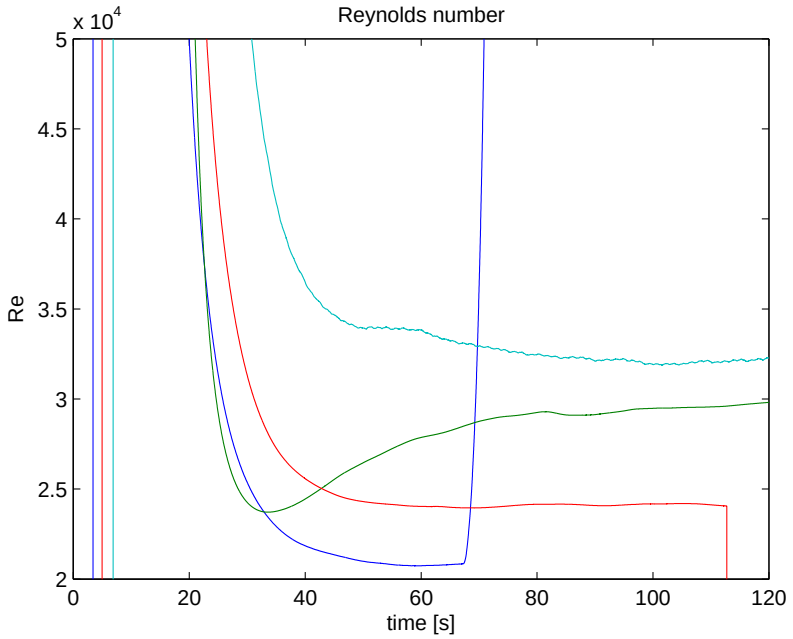

FIGURE 4.15: Reynolds number readings - 24 mm pipe diameter

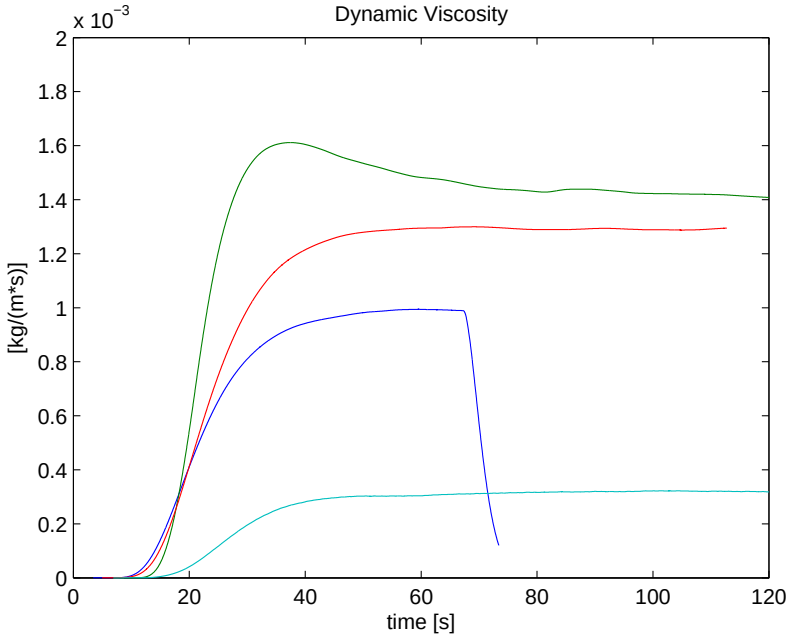

FIGURE 4.16: Dynamic viscosity readings - 24 mm pipe diameter

4.1.3 Differential Pressure Tests Through 12 mm Pipe

It could only be perform three different tests for the smallest pipe diameter. The reason for this is the sensors range, as mention in previous section, and the restriction of the pump. The pump itself can not be set lower than 0.03%. The reason for this, is that the motor do not get enough start power to begin rotating. Table 4.3 refers to the pump characteristics and their color represented in the plots. The time range of the recorded data is varying from 90 sec to 120 sec.

% of maximum pump rate	0.03	0.04	0.05
color	blue	green	red

TABLE 4.3: Colors represent the different flow rates in 12 mm diameter pipe

The pressure loss in the pipe is higher for smaller diameter due to the pipe friction against the wall. This resulted in high pressure readings for low flow rates as shown in Figure 4.18 for the horizontal section, and Figure 4.20 for the vertical section. Comparing all dimension, it can be seen that the dynamic fluid pressure loss (2.4) is stable around 10 mBar. The differential pressure in both horizontal and vertical section shows too low values according to theoretical values. An interesting observation shows that the results from differential-pressure readings at 0.05% are equal to the theoretical values at 0.04%. Similar observations can be detected for measurements at 0.04% and 0.03%, compared to theoretical values at 0.03% and 0.02%. This can indicate that the motor pump is not reliable for small flow rates, and give false flow rate out. The density measurements from Figure 4.21 is close up to the true density of water, and have a very small spread when reached stable flow. Since the differential-pressure measurements are not correct at given theoretical values, will the following results for the friction factor, Reynolds number and the viscosity be incorrect. The data for these values are found at Figure 4.22, Figure 4.23 and Figure 4.24 respectively.

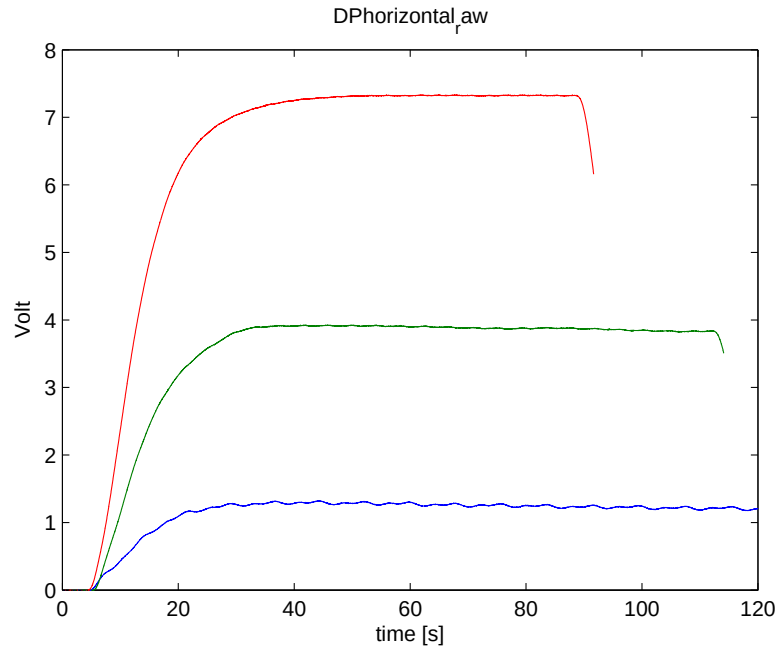

FIGURE 4.17: Voltage readings in horizontal line 12 - mm pipe diameter

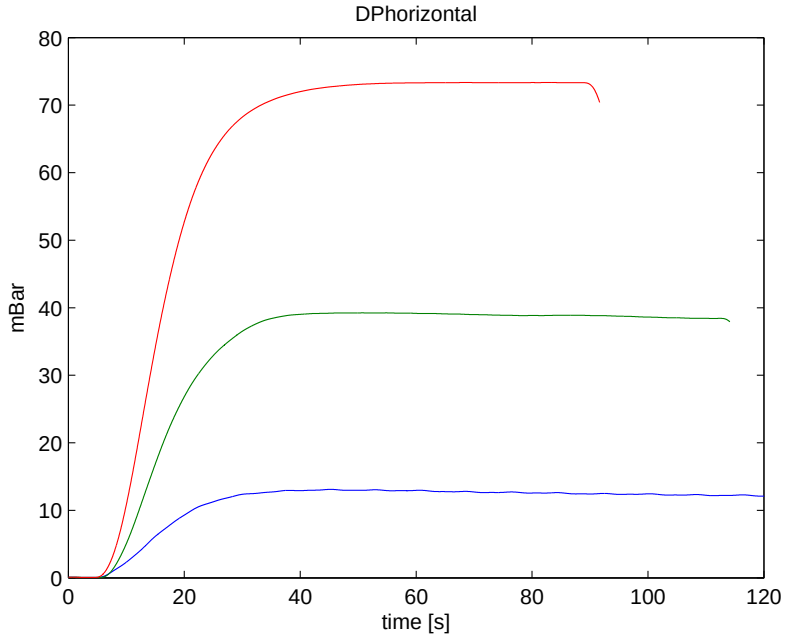

FIGURE 4.18: mBar in horizontal line 12 - mm pipe diameter

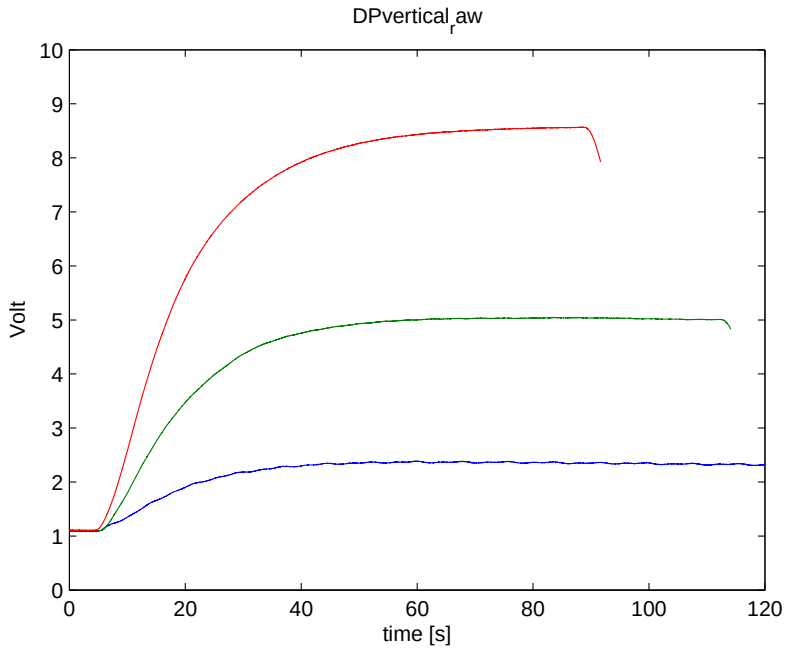

FIGURE 4.19: Voltage readings in vertical line - 12 mm pipe diameter

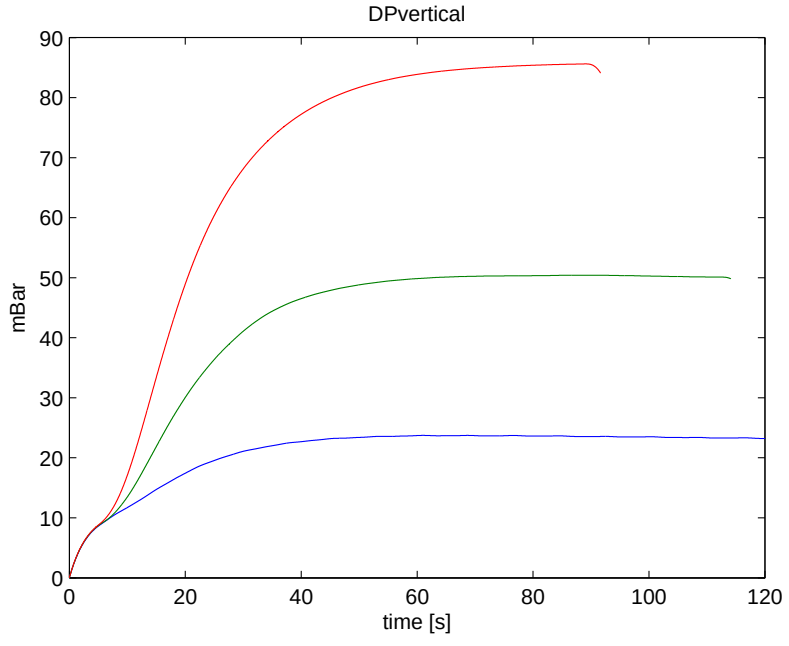

FIGURE 4.20: mBar in vertical line - 12 mm pipe diameter

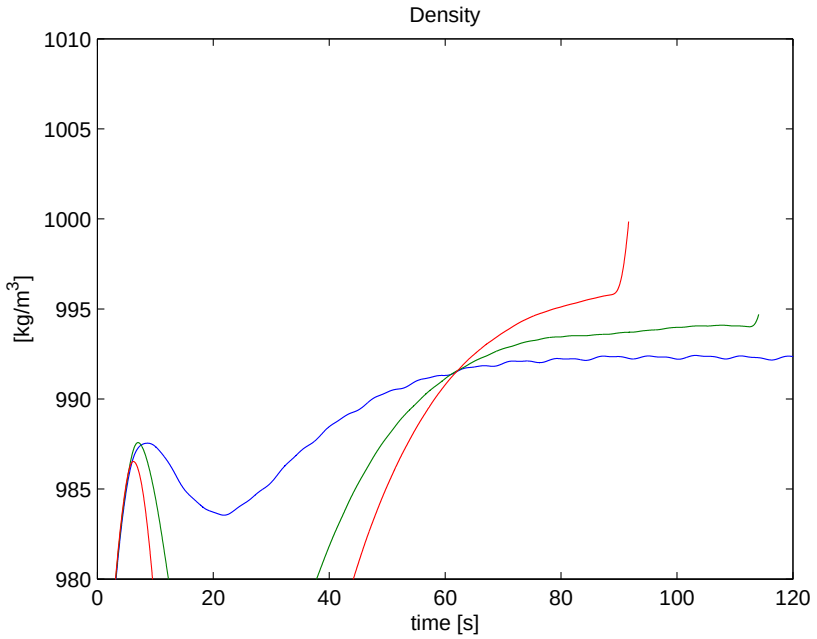

FIGURE 4.21: Density readings - 12 mm pipe diameter

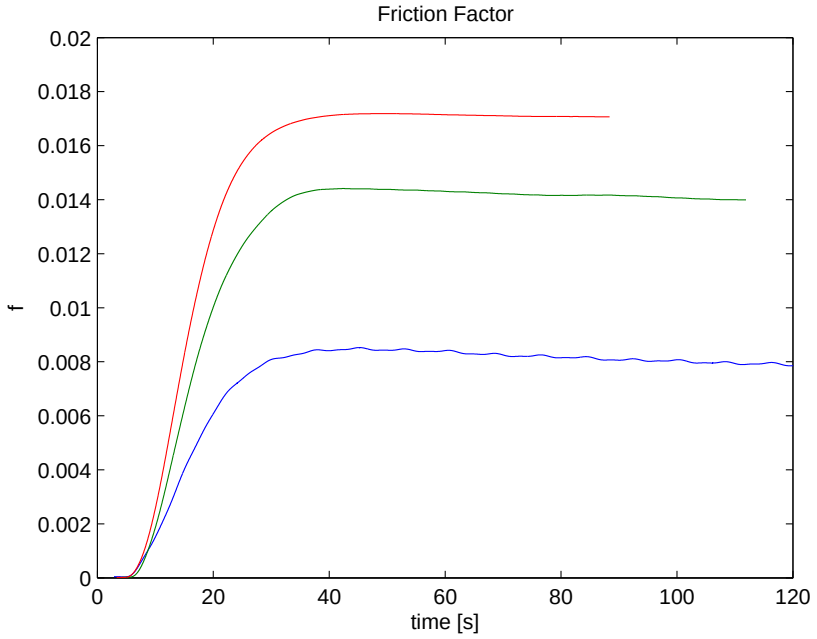

FIGURE 4.22: Friction factor readings - 12 mm pipe diameter

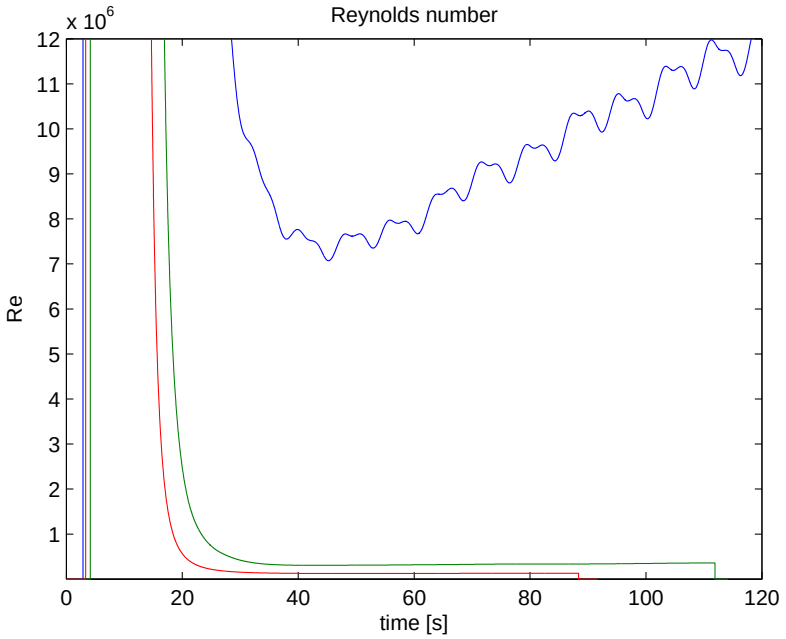

FIGURE 4.23: Reynolds number readings - 12 mm pipe diameter

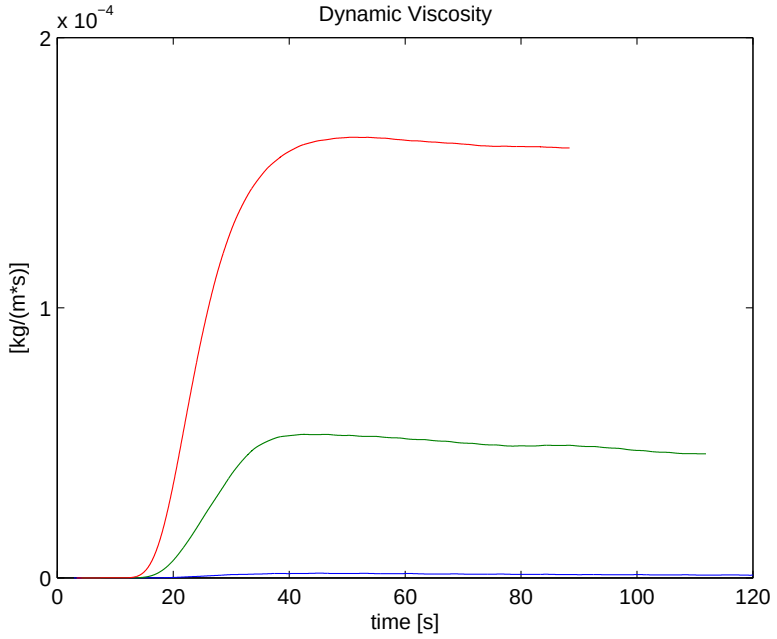

FIGURE 4.24: Dynamic viscosity readings - 12 mm pipe diameter

Chapter 5

Discussion of the experimental results

Automated drilling requires accurate and continuous drilling-fluid properties measurements. This section take the discussion if differential-pressure measurements are reliable to evaluate the drilling-fluid properties on the basis of the results given in this thesis.

The most important factor to highlight is that with differential-pressure measurements, the friction factor can be calculated regardless of the state of the flow. Neither the turbulent flow nor the laminar flow is a factor to the differential-pressure measurements. In theory this should be a reliable source of estimating the drilling-fluid properties.

5.1 Comparison of Theoretical Values and Measured Values

The majority of the density measurements were below the theoretical value of 998.2 kg/m^3. The given density value of the oil in the diaphragm cells from the vendor is 960 kg/m^3. This should give a result for P_d = 13.11 mBar. The measured P_d had an average value of ≈10. From this it can be assumed that actually ρ_o is 969 kg/m^3. If this is implied, would most of the density measurements be equal to true theoretical values.

It seemed that the best measurements for the horizontal section were achieved with pump rates between 0.1% and 0.2% of maximum pump pressure. At flow rates beneath 0.1% , the uncertainty were increased for the measurements, especially for 12 mm pipe diameter. This can indicate that the assumption of equation (4.1) is incorrect for low pump characteristics. Due to the restriction of the pump at low pump rates, the desired amount of test data with different flow rates could not be achieved.

If the flow rate were measured accurately with a Coriolis flow meter on the suction side, would the calculation of the friction factor be more accurate. At current state, are the flow rate measurements too uncertain by computing it from the % of maximum pump pressure. In addition, a new pump should be added to the laboratory. The pump should be designed to give low flow rates with minimal pulsation.

5.1.1 Evaluation of diaphragm sensors for differential-pressure measurement

The sensors gave stable data feed throughout the test phase. Even with low differential-pressure measurements, especially during the tests on 50 mm pipe diameter, it had very little disturbance. Compared to the differential-pressure results Hansen [4] measured at the flow loop, are the results from the diaphragm sensors very positive. If it is possible to test with a new pump and have a Coriolis flow meter on the suction side, would the test results be more true to theoretical values.

Chapter 6

Conclusion and future directions

The Instrumental Circulation Path has the potential to become a success to estimate drilling fluid properties. But the necessary equipment to perform a stable test is currently not in place. The uncertainties around the flow rate are too high to draw a clear conclusion to rely on. Concerning the test results, it gave some decent values to indicate the properties of water. Although some measurements could be discarded, it also showed that for some data values the approximation of water properties could be concluded.

The implementation of the diaphragm sensors can be seen as a success. They gave stable output values for both high and low differential-pressures. The next phase to make the Instrumental Circulation Path reliable to give acceptable data, is to ensure the correct output of the flow rate. As discussed in Chapter 5, a new pump and a Coriolis flow meter must be added to the facility. When this is established, can future test be performed with different types of drilling fluids with non-Newtonian properties.

Appendix A

Operating Procedures

Startup

1. Ensure the tank is filled up with liquid.
2. Close the valve connected to the other flow loop.
3. Close all valves related to the Circulation Path.
4. Mount the diaphragms at desired pipe diameter.
5. Open valve to the pipe diameter selected.
6. Ensure all extension cords are connected.
7. Run "datafil" in Matlab.
8. Start up "difftest" in Simulink.
9. Select correct pipe diameter in Simulink - /maling/Subsystem4.
10. Compile and connect to target.
11. Start the process with preferred settings.
12. Run until a stable flow have been reached

Shutdown

1. Stop the system.
2. Drain the water from the Circulation Path.

3. Open all valves.
4. Unplug extension cords.
5. Extract data from Matlab.
6. Shut down computer.
7. Clean up potential spills.

Appendix B

Technical documentation related to the Instrumental Circulating Path

Table of analogue input ports on control card PCI (6221)

Innganger	Kanalnr	Skilleforsterkerkort	Tilkobling	Signaltype
PT101	0	G1	68, 67	Analog
PT102	8	G2	34, 67	Analog
PT103	1	G3	33, 32	Analog
PT201	9	G4	66, 32	Analog
PT202	2	G5	65, 64	Analog
PT203	10	G6	31, 64	Analog
PT204	3	G7	30, 29	Analog
Tilbakemeld MPD-ventil	4	G8	28, 27	Analog
Tilbakemeld WCV-ventil	12	G9	61, 27	Analog
Motor monitorering	5		60, 59	Analog
DP1	6	G12	25, 24	Analog
DP2	14	G13	58, 24	Analog
dPv	7	G14	57, 24	Analog
dPh	15	G15	23, 24	Analog

Terminal blocks located at the middle in the communication cabinet

Number	Color	Signal	Type of equipment
7	White	-	dPv
8	Black	+	dPv
9	White	-	dPh
10	Black	+	dPh

Appendix C

Matlab codes

C.1 Headloss plot

```
close all


q = [1:100];
q = q./60000;    % Flow Rate [l/min] to [m^3/s]
visc = [1:100];
visc = visc./1000; %Pa*s]
for i = 1:length(q)
    for j = 1:length(visc)

% --- Define constants for the system and its components
L = 3.5;                % Pipe length [m]
D = 0.050;           % Pipe diameter [m]
A = 0.25*pi*D^2;     % Cross sectional area [m^2]
e = 0.0015e-3;       % Roughness for drawn tubing
rho = 1000;          % Density [kg/m^3]
g = 9.81;            % Acceleration of gravity [m^2/s]




mu = visc(j);       % Dynamic viscosity [kg/(m*s )]
nu =  mu/rho;       % Kinematic viscosity [m^2/s]
Q = q(i);           % [m^3/s]
V = Q/A;             % Velocity [m/s] ]

% --- Laminar solution
Re = V*D/nu;
flam = 64/Re;
dplam = flam * 0.5*(L/D)*rho*V^2;

% --- Turbulent solution
f = moody(e/D,Re);
```

```
dp = f*(L/D)*0.5*rho*V^2;

pipefric(i,j) = dp;

    end
end

figure
plot(visc);
title('viscosity range');
xlabel('m^2/s');
ylabel('kg/(ms)');

figure;
plot(q);
title('flow range');
xlabel('l/min');
ylabel('m^3/s');

figure;
plot(pipefric);
title('pipe friction')
xlabel('l/min');
ylabel('Pa');

figure;
mesh(visc,q,pipefric);
xlabel('m^2/s');
ylabel('m^3/s');
zlabel('Pa');

figure;
plot(q,pipefric)
title('q V dP')
xlabel('m^3/s');
ylabel('Pa');


% --- Summary of losses
fprintf('\nReynolds Number: Re = %12.3e\n\n',Re);
fprintf('\tLaminar flow:   ');
fprintf('flam = %8.5f;   Dp = %7.0f (Pa)\n',flam,dplam)
fprintf('\tTurbulent flow: ');
fprintf('f    = %8.5f;   Dp = %7.0f (Pa)\n',f,dp);
```

```
function f = moody(ed,Re,verbose)

if Re<0
  error(sprintf('Reynolds number = %f cannot be negative',Re));
elseif Re<2000
  f = 64/Re;  return      %  laminar flow
end
if ed>0.05
  warning(sprintf('epsilon/diameter ratio = %f is not on Moody chart',ed));
end
```

```
if Re<4000, warning ('Re = %f in transition range ',Re);
end

findf = inline('1.0/sqrt(f) + 2.0*log10( ed/3.7 + 2.51/( Re*sqrt(f)) )','f','ed','Re');
fi = 1/(1.8*log10(6.9/Re + (ed/3.7)^1.11))^2;   %  initial guess at f
dfTol = 5e-6;
f = fzero(findf,fi,optimset('TolX',dfTol,'Display','off'),ed,Re);
% --- sanity check:
if f<0, error(sprintf('Friction factor = %f, but cannot be negative',f));
end
```

C.2 Fluid properties

```
close all


g = 9.81;    % Acceleration of gravity [m^2/s]
rhoo = 960;   % Density [kg/m^3]
h = 3.5;
L = 3.5;                % Pipe length [m]
D = 0.050;              % Pipe diameter [m]
A = 0.25*pi*D^2;        % Cross sectional area [m^2]
e = 0;                  %0.0015e-3;       % Roughness for drawn tubing
t = Difftrykk.time;

dPhor = (Difftrykk.signals(2).values)*100;   % Differential Pressure [Pa]
dPver = (Difftrykk.signals(1).values)*100;   % Differential Pressure [Pa]


%Q = 0.04*(14/3600);
Q = regulering.signals(1).values.*(14/3600);% Flow Rate [l/min] to [m^3/s]
V = Q'/A ;            % Velocity [m/s]
rhol = rhoo+((dPver'-dPhor')/(g*h));

f2 =2*D*dPhor';
f3 =rhol'.*V'.^2*L;

f = (f3)'/(f4)';

Re = (2.51)/(sqrt(f')*(10^(-1.0/(2.0*sqrt(f'))))-((e/D)/3.7)));

mu = (rhol'*V*D)/Re';

figure;
plot(f4);

figure;
plot(t,dPver);
title('dPvertical');
xlabel('time [s]');
ylabel('Pa');
```

```
figure;
plot(t,dPhor);
title('dPhorizontal');
xlabel('time [s]');
ylabel('Pa');

figure;
plot(t,rhol);
title('Density');
xlabel('time [s]');
ylabel('[kg/m^3]');

%figure;
%plot(t,f);
%title('Friction Factor');
%xlabel('time [s]');
%ylabel('f');

figure;
plot(t,mu);
title('Dynamic Viscosity');
xlabel('time [s]');
ylabel('[kg/(m*s)]');

figure;
plot(t,Re);
title('Reynolds number');
xlabel('time [s]');
ylabel('Re');
```

Bibliography

[1] Liv A. Carlsen. Simultaneous continuous monitoring of the drilling-fluid friction factor and density. *SPE Paper*, 1(1):34–44, March 2013.

[2] Magnus Tveit Torsvik. Laboratory model of well drilling process. construction, instrumentation, startup and regulation. *Master thesis*, 1(1):1–91, June 2011.

[3] Alexander Wang. Mpd og automatisk brnnsparkhndtering anvendt p boreriggmodell. *Master thesis*, 1(1):1–98, January 2012.

[4] Erik Hansen. Automatic evaluation of drilling fluid properties. *Master's Thesis*, 1(1):1–92, June 2012. URL http://brage.bibsys.no/uis/handle/URN:NBN:no-bibsys_brage_34884.

[5] Gerhard Nygaard and John-Morten Godhavn. Automated drilling operations. *Compendium*, 1(1):23–26, April 2013.

[6] Autodesk inventor professional 2013. *Compendium*, 1:–. URL http://www.students.autodesk.com/.